Elastohydrodynamics of Towed Slender Bodies: the Effect of Nose and Tail Shapes on Stability

Michael P. Paidoussis* and Byung-Kun Yu†
McGill University, Montreal, Canada

A general theory is presented to account for the dynamics and stability of a slender flexible body with a rounded nose section and a truncated rounded tail section, towed underwater. Particular attention is focused on the hydrodynamic forces acting on the two extremities of the body, which are determined by means of ideal flow theory, rather than by slender body theory. To this end, general expressions were obtained for the forces and moments acting on an ellipsoid undergoing planar motions. Sufficient results are presented to illustrate 1) the dynamical behavior of the body with increasing towing speed, and 2) the effect of some parameters, such as the shape of the ends, on stability. It was found that stability is mainly controlled by the shape of the tail section of the body.

Nomenclature‡

a,b	= defined following Eq. (A4)
C_{DB}	= base drag coefficient
c_f	= friction coefficient
D,D_B	= diameter of cylinder and of base of the body
$D(\xi)$	= local diameter of the body
EI	= flexural rigidity of the body
e	= eccentricity of ellipsoid
F_n,F_ℓ	= normal and longitudinal viscous forces on the body, per unit length
f_1,f_2	= slenderness coefficients for hydrodynamic forces at free ends
I_n,I_ℓ	= normal and longitudinal inviscid hydrodynamic forces on the body, per unit length
k_1,k_2,ℓ_3	= defined by Eq. (A14) and (A11)
L	= length of main body
m,M	= mass and virtual mass of the body, per unit length
P,P_n,P_ℓ	= tow-rope forces defined by Fig. 1
Q	= shear force at a cross section of the body
$S_{\max},S_B$	= maximum and base surface areas of the body
s	= length of tow-rope
T	= tension
t	= time
U	= mean flow velocity
u	= dimensionless flow velocity $=(M/EI)^{1/2}UL$
x	= axial coordinate
x'	= spheroidal coordinates defined by Eq. (A4)
y	= lateral displacement of the body
α	= bluntness of tail portion $=\lambda_2/\lambda_1$
β	$=M/(m+M)$
γ,δ	= angles defined by Fig. 1
ϵ	$=L/D$
η	$=y/L$
Λ	$=s/L$
$\mathfrak{M}$	= moment on a cross section of the body
ξ	$=x/L$
ρ	= fluid density
τ,τ'	$=Ut/L$ and $\{EI/(m+M)\}^{1/2}t/L^2$, respectively
Ω	= circular natural frequency
ω	= dimensionless natural frequency $=\{(m+M)/EI\}^{1/2}\Omega L^2$

Received Jan. 5, 1976; revision received April 7, 1976. This research was sponsored by the Defence Research Board of Canada, whose support is gratefully acknowledged.

Index categories: Hydrodynamics; Marine Vessel Systems, Submerged; Aeroelasticity and Hydroelasticity.

*Associate Professor, Department of Mechanical Engineering.

†Research Assistant, Department of Mechanical Engineering.

‡Note: In this paper, bold superscripted numerals on mathematical symbols are indices and not powers, e.g., x^2; $[x^2]^2 = x^2x^2 \neq x^4$

I. Introduction

INTEREST in the dynamics of flexible towed slender bodies began with the development of the Dracone flexible barge for the transportation of fluids lighter than sea water. The first study on the stability of such systems was undertaken by Hawthorne.[1] Later, a more comprehensive dynamical analysis, supported by experiment, was presented by Paidoussis,[2,3] for flexible cylindrical bodies with streamlined ends towed underwater. Pao[4] further extended this work.

It was found that such systems are subject to two classes of instability: essentially rigid-body instabilities, which manifest themselves at low towing speeds and can be either oscillatory or nonoscillatory; and flexural instabilities, which occur at higher towing speeds, and involve either flutter or divergence (buckling) of the towed cylinder. It was found that, in general, as the towing speed is increased, a towed system is subject to several of these instabilities, either sequentially or concurrently. Means for stabilizing the system with respect to one form of instability generally were found to be effective with respect to other forms of instability. Such means were mainly related to the tow-rope length or the shapes of the nose and tail of the body; indeed it was found that the overall stability of the system could be controlled effectively by the shapes of the nose and tail sections of the body.

In the aforementioned studies, the hydrodynamic forces acting on the main, cylindrical part of the body were determined by means of slender body theory, and those acting on the nose and tail were dealt with by using the same expressions modified by semiempirical correction factors. The main contribution of this paper is to account carefully for the hydrodynamic forces on the nose and tail by means of ideal flow theory, by evaluating the forces and moments acting on an ellipsoid, which is undergoing general planar motion (Appendix A). At the same time, several other improvements in the formulation of the equations of motion have been incorporated.

Apart from its intrinsic interest, practical interest in this work is not confined to the Dracone barge, which is almost but not completely submerged, but also to recently proposed underwater transportation systems involving rigid cylindrical containers coupled elastically in a chain-like fashion.[5]

II. Forces Acting on a Towed Slender Body

Consider a slender body or revolution immersed in an incompressible fluid of density ρ, flowing with uniform velocity U parallel to the x axis, which coincides with the position of rest of the body and of the tow-rope, as shown in Fig. 1. It is noted that this is exactly equivalent to the body being towed with velocity U in still fluid. The x and y axes lie in a horizontal plane wherein all motions $y(x,t)$ should be confined. Also,

it is assumed that the body is of null buoyancy and uniform density, so that neither lateral forces nor moments are necessary to keep it lying along the x axis, at least at zero flow velocity.

Before proceeding with the analysis, it is desirable to define the following dimensionless terms:

$$\xi = x/L \qquad \eta = y/L \qquad \tau = Ut/L \tag{1}$$

For the sake of analysis, the body is divided into three parts. The main portion of the body extends from $\xi = -\frac{1}{2}$ to $\xi = \frac{1}{2}$. The length of the nose and tail ℓ_1 and ℓ_2 may be non-dimensionalized as $\lambda_1 = \ell_1/L$ and $\lambda_2 = \ell_2/L$, respectively; these quantities are considered to be small, thus allowing considerable simplification of the kinematics of the nose and tail. Thus, along the nose, $\eta(\xi,\tau)$ may be represented adequately by

$$\eta(\xi,\tau) = \eta_1(\tau) + (\xi + \tfrac{1}{2})\theta_1(\tau) \tag{2}$$

where

$$\eta_1(\tau) = \eta(-\tfrac{1}{2},\tau) \text{ and } \theta_1(\tau) = \partial\eta/\partial\xi|_{\xi=-\frac{1}{2}}$$

Similarly, for the tail one may write

$$\eta(\xi,\tau) = \eta_2(\tau) + (\xi - \tfrac{1}{2})\theta_2(\tau) \tag{3}$$

Now, let us consider the hydrodynamic forces acting on the main part of the body. For turbulent boundary layers, Taylor[6] proposed that the normal and longitudinal components of the viscous force may be expressed as follows:

$$\begin{aligned} F_n &= \tfrac{1}{2}\rho U^2 c_f [S(\xi)/D(\xi)]\,(\partial\eta/\partial\tau + \partial\eta/\partial\xi) \\ F_\ell &= \tfrac{1}{2}\rho U^2 c_f [S(\xi)/D(\xi)] \end{aligned} \tag{4}$$

According to Lighthill's work,[7] the normal and longitudinal components of the inviscid hydrodynamic force per unit length of the deformed body, obtained by means of slender body theory, are

$$\begin{aligned} I_n &= \frac{\rho U^2 S(\xi)}{L}\left[\frac{\partial}{\partial\tau} + \frac{\partial}{\partial\xi}\right]^2 \eta + \frac{\rho U^2}{L}\frac{dS(\xi)}{d\xi}\left[\frac{\partial\eta}{\partial\tau} + \frac{\partial\eta}{\partial\xi}\right] \\ I_\ell &= 0 \end{aligned} \tag{5}$$

respectively. Unfortunately, the previous expressions are valid only over those portions of the body for which $dD(\xi)/d\xi$ is small, which clearly is not the case for the nose and tail sections of the body.

In order to deal with the forces acting on nonslender portions of the body, use is made of ideal flow theory, without the restrictive assumptions of slender body theory. In Appendix A expressions are developed for the inviscid hydrodynamic forces on an ellipsoid of revolution undergoing general motion. For the nose, these forces per unit length are given by

$$\begin{aligned} I_n = \frac{-\rho U^2 S(\xi)}{L}\Bigg[&\left\{\frac{d^2\eta_1}{d\tau^2} + (\xi+\tfrac{1}{2})\frac{d^2\theta_1}{d\tau^2} + \frac{d\theta_1}{d\tau}\right\}k_2 \\ &- \left\{\frac{d\eta_1}{d\tau} + (\xi+\tfrac{1}{2})\frac{d\theta_1}{d\tau} + \theta_1\right\}\frac{L}{a}(1+k_1)(1+k_2)\frac{x^2}{1-e^2[x^2]^2} \\ &+ \frac{d^2\theta_1}{d\tau^2}\frac{a}{L}\ell_3 x^2 - \frac{d\theta_1}{d\tau}\left\{\frac{(1+k_1)(1+\ell_3(2[x^2]^2-1))}{1-e^2[x^2]^2} - 1\right\}\Bigg] \end{aligned}$$

$$I_\ell = \rho U^2 S_{\max}\frac{x^2}{a}\left[\frac{(1+k_1)^2(1-[x^2]^2)}{1-e^2[x^2]^2} - 1\right] \tag{6}$$

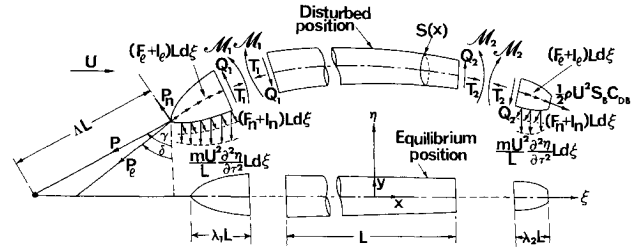

Fig. 1 A diagram of a slender body towed underwater, showing the four components: the tow-rope, the "nose", the slender (main) portion of the body, and the "tail."

where $S_{\max}$ is the maximum cross section of the ellipsoid, e its eccentricity, x^2 is the second spheroidal coordinate (Fig. A1), and a, k_1, k_2, and ℓ_3 are given in Appendix A.

In case the nose is not an ellipsoid, it still may be analyzed by means of the previous expressions by considering the forces at each point to be approximately equal to those acting on an equivalent ellipsoid, according to the technique developed by Upson and Klikoff[8]; in such a case, a, k_1, x^2, etc. become functions of ξ.

The tail section presents more difficulties because of possible flow separation, the circumferential location of which would shift with movements of the body. For the purposes of this analysis it is assumed that the tail is truncated at a point, such that separation does not occur before it; this is likely to be the case anyway, since it was found that a relatively blunt tail has a very important stabilizing effect on the system.[2,3] In such a case, clearly the same sort of analysis as for the nose may be applied and, accordingly, one finds

$$\begin{aligned} I_n = \frac{\rho U^2 S(\xi)}{L}\Bigg[&\left\{\frac{d^2\eta_2}{d\tau^2} + (\xi-\tfrac{1}{2})\frac{d^2\theta_2}{d\tau^2} + \frac{d\theta_2}{d\tau}\right\}k_2 \\ &- \left\{\frac{d\eta_2}{d\tau} + (\xi-\tfrac{1}{2})\frac{d\theta_2}{d\tau} + \theta_2\right\}\frac{L}{a}(1+k_1)(1+k_2)\frac{x^2}{1-e^2[x^2]^2} \\ &+ \frac{d^2\theta_2}{d\tau^2}\frac{a}{L}\ell_3 x^2 - \frac{d\theta_2}{d\tau}\left\{\frac{(1+k_1)\{1+\ell_3(2[x^2]^2-1)\}}{1-e^2[x^2]^2} - 1\right\}\Bigg] \end{aligned}$$

$$I_\ell = \rho U^2 S_{\max}\frac{x^2}{a}\left[\frac{(1+k_1)^2(1-[x^2]^2)}{1-e^2[x^2]^2} - 1\right] \tag{7}$$

for the inviscid hydrodynamic forces on the tail, per unit length.

Finally, there will be a force due to base drag acting on the tail; following Hoerner,[9] the base drag may be expressed as

$$\mathfrak{D}_B = \tfrac{1}{2}\rho U^2 S_B C_{DB} \tag{8a}$$

with the base drag coefficient given by

$$C_{DB} = 0.029\,(\tfrac{1}{2}\rho U^2 S_B/\mathfrak{D}_{\text{fore}})^{\frac{1}{2}} \tag{8b}$$

where $\mathfrak{D}_{\text{fore}}$ is the total drag acting over the entire forebody.

III. Equations of Motion and Boundary Conditions

Consider a small element $\delta\xi$ of the body undergoing small free lateral motions, as shown in Fig. 2. Taking force balances in the ξ and η direction and a moment balance, one obtains

$$\frac{\partial T}{\partial\xi} + F_\ell L + (F_n + I_n)L\left(\frac{\partial\eta}{\partial\tau} + \frac{\partial\eta}{\partial\xi}\right) = 0 \tag{9}$$

$$\frac{\partial Q}{\partial\xi} - (F_n + I_n)L + \frac{\partial}{\partial\xi}\left(T\frac{\partial\eta}{\partial\xi}\right) + F_\ell L\frac{\partial\eta}{\partial\xi} - mU^2\frac{\partial^2\eta}{\partial\tau^2} = 0 \tag{10}$$

$$QL+\frac{\partial \mathfrak{M}}{\partial \xi}=0 \tag{11}$$

Henceforth, it will be assumed that the main portion of the body is a uniform cylinder, for the sake of simplicity. Substituting Eqs. (4) and (5) into Eq. (9), neglecting terms of second order in small quantities, and integrating from some arbitrary ξ to the point at which, the tail section begins, one obtains

$$T(\xi)=T_2+\tfrac{1}{2}\rho U^2 c_f(S/D)L(\tfrac{1}{2}-\xi) \tag{12}$$

where T_2 is the axial force exerted by the tail on the main portion of the body,

$$T_2=\int_{\frac{1}{2}}^{\frac{1}{2}+\lambda_2}(F_\ell+I_\ell)Ld\xi+\tfrac{1}{2}\rho U^2 S_B C_{DB}$$

where F_ℓ and I_ℓ are given by Eqs. (4) and (7). If in turn Eq. (12), along with Eqs. (4) and (5), are substituted into Eq. (10) and Eq. (9) is used one obtains

$$-\frac{\partial Q}{\partial \xi}+\rho U^2 S\left[\frac{\partial}{\partial \tau}+\frac{\partial}{\partial \xi}\right]^2\eta+\tfrac{1}{2}\rho U^2 c_f\frac{S}{D}L\left(\frac{\partial \eta}{\partial \tau}+\frac{\partial \eta}{\partial \xi}\right)$$

$$-[T_2+\tfrac{1}{2}\rho U^2 c_f(S/D)L(\tfrac{1}{2}-\xi)]\frac{\partial^2\eta}{\partial \xi^2}+mU^2\frac{\partial^2\eta}{\partial \tau^2}=0 \tag{13}$$

Finally, using Eq. (11) and the relationship

$$\mathfrak{M}=\frac{EI}{L}\frac{\partial^2\eta}{\partial \xi^2} \tag{14}$$

and substituting into Eq. (13), one obtains the equation of small lateral motions.

The boundary conditions at $\xi=-\frac{1}{2}$ and $\frac{1}{2}$ are determined by integrating the forces and moments acting on the nose and tail. Thus, the shear force Q_2 may be expressed as

$$Q_2\equiv-\frac{EI}{L^2}\frac{\partial^3\eta}{\partial \xi^3}\bigg|_{\xi=\frac{1}{2}}=-\int_{\frac{1}{2}}^{\frac{1}{2}+\lambda_2}(F_n+I_n+\frac{mU^2}{L}\frac{\partial^2\eta}{\partial \tau^2})Ld\xi \tag{15}$$

with F_n and I_n given by Eqs. (4) and (7); and the moment $\mathfrak{M}_2$ is given by

$$\mathfrak{M}_2\equiv\frac{EI}{L}\frac{\partial^2\eta}{\partial \xi^2}\bigg|_{\xi=\frac{1}{2}}=-\int_{\frac{1}{2}}^{\frac{1}{2}+\lambda_2}L(\xi-\tfrac{1}{2})\left(F_n+I_n+\frac{mU^2}{L}\frac{\partial^2\eta}{\partial \tau^2}\right)Ld\xi$$

$$+\int_{\frac{1}{2}}^{\frac{1}{2}+\lambda_2}\frac{b^2}{a}x^2 I_n L d\xi\simeq 0 \tag{16}$$

Before proceeding with the determination of the boundary conditions at $\xi=-\frac{1}{2}$, it is noted that the normal force due to the tow-rope (Fig. 1) is given by

$$P_n=P_\ell\tan(\gamma-\delta)=P_\ell\left(\frac{\partial \eta}{\partial \xi}-\frac{\eta}{\Lambda}\right)\bigg|_{\xi=-\frac{1}{2}-\lambda_1}$$

$$=P_\ell(\theta_1-\frac{\eta_1-\theta_1\lambda_1}{\Lambda}) \tag{17}$$

where the familiar trigonometric identities were used, as well as perturbation expansions for $\partial\eta/\partial\xi$ and η/Λ, and where

$$P_\ell=T_2+\tfrac{1}{2}\rho U^2(S/D)Lc_f+\int_{-\frac{1}{2}-\lambda_1}^{-\frac{1}{2}}(F_\ell+I_\ell)Ld\xi$$

Hence, one may obtain

$$Q_1\equiv-\frac{EI}{L^2}\frac{\partial^3\eta}{\partial \xi^3}\bigg|_{\xi=-\frac{1}{2}}$$

$$=-P_n+\int_{-\frac{1}{2}-\lambda_1}^{-\frac{1}{2}}\left(F_n+I_n+\frac{mU^2}{L}\frac{\partial^2\eta}{\partial \tau^2}\right)Ld\xi \tag{18}$$

$$\mathfrak{M}_1\equiv\frac{EI}{L}\frac{\partial^2\eta}{\partial \xi^2}\bigg|_{\xi=-\frac{1}{2}}=\lambda_1 LP_n$$

$$+\int_{-\frac{1}{2}-\lambda_1}^{-\frac{1}{2}}L(\xi+\tfrac{1}{2})\left(F_n+I_n+\frac{mU^2}{L}\frac{\partial^2\eta}{\partial \tau^2}\right)Ld\xi$$

$$-\int_{-\frac{1}{2}-\lambda_1}^{-\frac{1}{2}}\frac{b^2}{a}x^2 I_n L d\xi \tag{19}$$

where I_n and I_ℓ are given by Eq. (6).

The integrals in Eqs. (15, 16, 18, and 19) may be expressed conveniently in terms of a number of smaller integrals, which are functions of the shape of the nose and tail. As an illustration, consider Eq. (19) in its full form

$$\frac{EI}{L}\frac{\partial^2\eta}{\partial \xi^2}=L\lambda_1\tfrac{1}{2}\rho U^2 S_{\max}\{\epsilon c_f(i_{110}+i_{120}+I)$$

$$+2(i_{710}+i_{720})+\frac{S_B}{S_{\max}}C_{DB}\}\ (\theta_1-\frac{\eta_1-\theta_1\lambda_1}{\Lambda})$$

where

$$i_{110}=\frac{D_{\max}}{S_{\max}}\int_{-\frac{1}{2}-\lambda_1}^{-\frac{1}{2}}\frac{S(\xi)}{D(\xi)}d\xi$$

$$i_{710}=\int_{-\frac{1}{2}-\lambda_1}^{-\frac{1}{2}}\frac{L}{a}x^2\left\{\frac{(1+k_1)^2(1-[x^2]^2)}{1-e^2[x^2]^2}-1\right\}d\xi$$

and i_{120} and i_{720} are equivalent expressions with the limits of integration being $\frac{1}{2}$ and $\frac{1}{2}+\lambda_2$.

IV. Analysis

Before proceeding with the analysis, the equation of motion and the boundary conditions are rendered completely dimensionless by defining

$$u=(\rho S/EI)^{\frac{1}{2}}UL \quad \text{and} \quad \beta=\rho S/(\rho S+m) \tag{20}$$

where $\beta=\frac{1}{2}$ throughout for null buoyancy. Furthermore, the dimensionless time

$$\tau'=[EI/(\rho S+m)]^{\frac{1}{2}}t/L^2=\beta^{\frac{1}{2}}\tau/u \tag{21}$$

is used, since the resultant flexural frequencies at $U=0$ then correspond to the frequencies of a free-free beam. Thus, the dynamics of the system depend on the parameters $u,\epsilon c_f,\Lambda,\lambda_1$, and λ_2. In cases in which the nose and tail are identical ellipsoids, but with the tail truncated, λ_2 may be expressed by $\lambda_2=\alpha\lambda_1$.

Let us now consider motions of the body of the form

$$\eta=Y(\xi)e^{i\omega\tau'}=\sum_{r=0}^{\infty}A_r(\xi+\tfrac{1}{2})^r e^{i\omega\tau'} \tag{22}$$

where ω is a dimensionless frequency, which is generally complex. Substituting this into the equation of motion, and collecting terms in powers of $(\xi+\frac{1}{2})$, it is found that all of the A_r may be expressed in terms of A_0,A_1,A_2, and A_3. Then, substituting into the boundary conditions, using the recurrence expressions found in the preceding, and truncating the series, the problem reduces to a matrix equation of the form

$$[G]\{A_0,A_1,A_2,A_3\}^T=\{0\}$$

which, for nontrivial solution, leads to $\det[G]=0$; this is an implicit expression for determing the eigenfrequencies of the system ω_i. If the imaginary part of one of the ω_i's is negative, $Im(\omega_j)<0$, this indicates that motions will be amplified. If

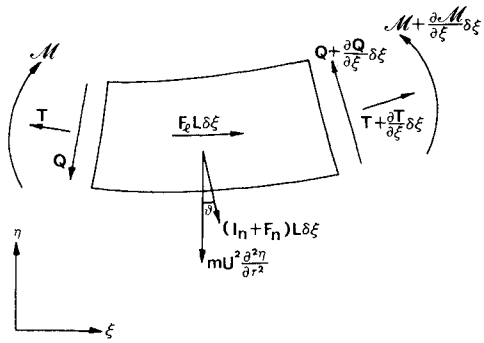

Fig. 2 An element, δx, of the main part of the body showing the forces and moments acting on it ($\vartheta \simeq \partial\eta/\partial\xi + \partial\eta/\partial\tau$).

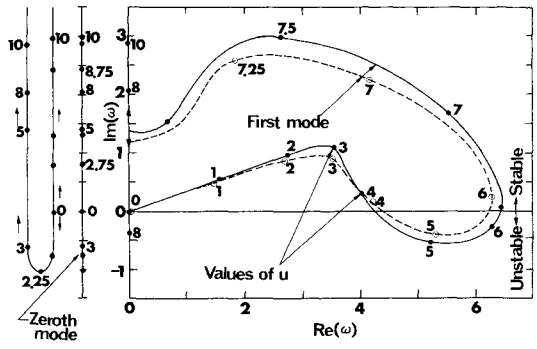

Fig. 3 The eigenfrequencies of the zeroth and first modes of a system ($\epsilon c_f = 1$, $\lambda_1 = 0.015$, $\Lambda = 5$, $\alpha = 1$) as functions of the towing speed, u. ——, this theory;---, older theory (with $f_1 = 0.6035, f_2 = 0.6046$).

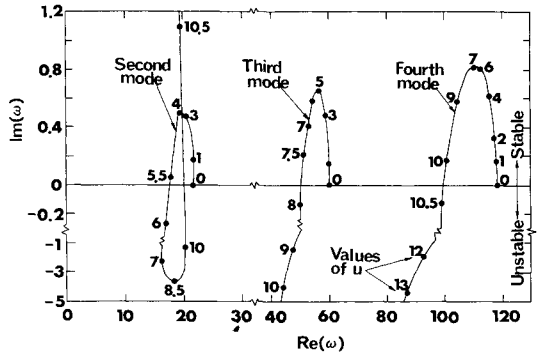

Fig. 4 The eigenfrequencies of the second, third, and fourth modes of the same system as in Fig. 3.

the corresponding real part $Re(\omega_j)$ is nonzero, then this implies an oscillatory (flutter) instability; and if it is zero, divergence is implied.

V. Results

A typical set of results for a uniform flexible cylinder with ellipsoidal ends is shown in Figs. 3 and 4, where the frequencies of the lowest five modes of the system are shown, plotted as Argand diagrams, with the dimensionless towing speed u as a parameter. It is seen that at low u the system is unstable by yawing (divergence) in its so-called zeroth mode; at the same time, towing is seen to generate flow-induced damping [$Im(\omega) > 0$] in the higher modes of the system. Then, at higher u, the system is subject to oscillatory instabilities (flutter) successively in its first, second, third, and fourth modes. These results are qualitatively similar to those obtained previously.[2,3]

It is instructive to consider the differences in the results obtained by this and previous theories, so as to obtain a measure of the effect of the refined manner in which the forces at the

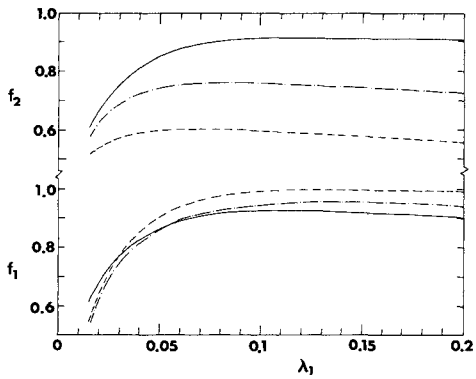

Fig. 5 The factors f_1 and f_2 of older theories related to the parameters of this, more refined, theory for $\epsilon c_f = 1$, $\Lambda = 1$. —— $\alpha = 1$; —·— $\alpha = 0.9$;---$\alpha = 0.8$.

extremities of the body have been dealt with here. To this end, the older theory[3] was modified to conform with the present theory in all respects, except for the boundary conditions, which incorporate the forces acting on the nose and tail of the body. It is noted that in the older theory the inviscid hydrodynamic forces were determined by slender-body theory, and departures from them were accounted for by incorporating semiempirical correction factors; thus, at the nose, the inviscid hydrodynamic forces were simply taken to be

$$-f_1 \frac{\rho U^2 S}{L}\left[\frac{\partial}{\partial\tau} + \frac{\partial}{\partial\xi}\right]^2 \eta$$

per unit length ($0 \le f_1 \le 1$), whereas at the tail the same form was taken, but with a factor f_2.

Clearly, by comparing the various terms in the old and the new sets of boundary conditions, one may relate f_1 and f_2 to the parameters associated with this (new) theory. This was done in Fig. 5 for a body with ellipsoidal ends, by comparing the coefficients of u^2 in the terms involving $dY/d\xi$ [cf., Eq. (22)] in the boundary conditions associated with shear at the ends. Here the parameter α is defined by

$$\alpha = \lambda_2/\lambda_1$$

and indicates the degree of truncation of the ellipsoid at the tail; thus, $\alpha = 0.75$ indicates that the tail is formed by an ellipsoid identical to that of the nose, truncated to three-quarters its original length. Thus, approximate values of f_1 and f_2 may be obtained for given ϵc_f, Λ and, of course, λ_1 and α.

Some calculations were conducted in which the results obtained by this theory are compared with those of the older theory, utilizing values of f_1 and f_2 from Fig. 5, and a form drag coefficient at the tail (in the older theory) $c_2 = (1\text{-}f_2)/2$. Typical results are shown in Fig. 6 for the second mode of the system and in Fig. 3 for the first mode. It is evident that, although the results obtained by the two theories are similar, they are by no means identical. This reflects the fact that two parameters (f_1 and f_2) are insufficient to account adequately for the refinements introduced by this theory; for instance, according to this theory there are different virtual masses for the nonuniform parts of the body, associated with different types of motions, whereas the older theory is based on slender-body considerations and assumes a single virtual mass for all "lateral" motions. It is of interest to note that, in the case of the first mode (Fig. 3), the correspondence of the two theories is quite good up to $u \simeq 5$; generally, agreement deteriorates with the complexity of motion (mode number) and with increasing u.

Next, consider the effect of some parameters on stability. Figures 7 and 8 show, respectively, the effect of the two-rope

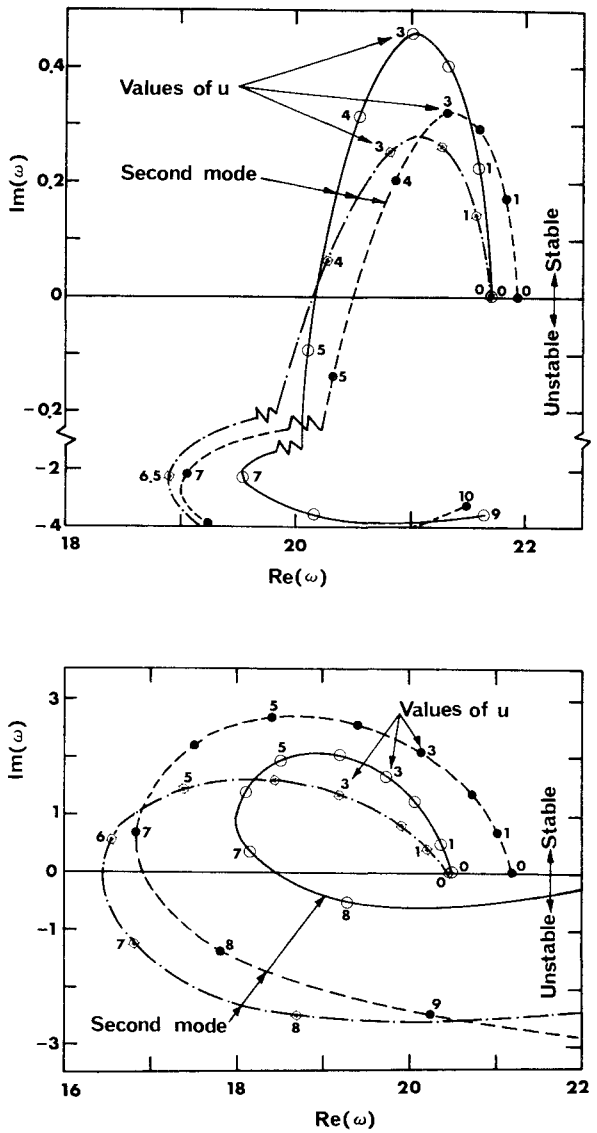

Fig. 6 The second-mode eigenfrequencies according to this and the older theories. Upper figure:---, this theory ($\lambda_1 = 0.015$, $\Lambda = 1$, $\epsilon c_f = 1$, $\alpha = 1$); —·— older thoery ($f_1 = 0.6034$, $f_2 = 0.6046$); — older theory ($f_1 = 0.6046$; $f_2 = 0.5500$). Lower figure: ---, this theory ($\lambda_1 = 0.045$, $\Lambda = 1$, $\epsilon c_f = 1$, $\alpha = 0.8$); —·—, older theory ($f_1 = 0.8839, f_2 = 0.6014$); —, older theory ($f_1 = 0.8839, f_2 = 0.5000$).

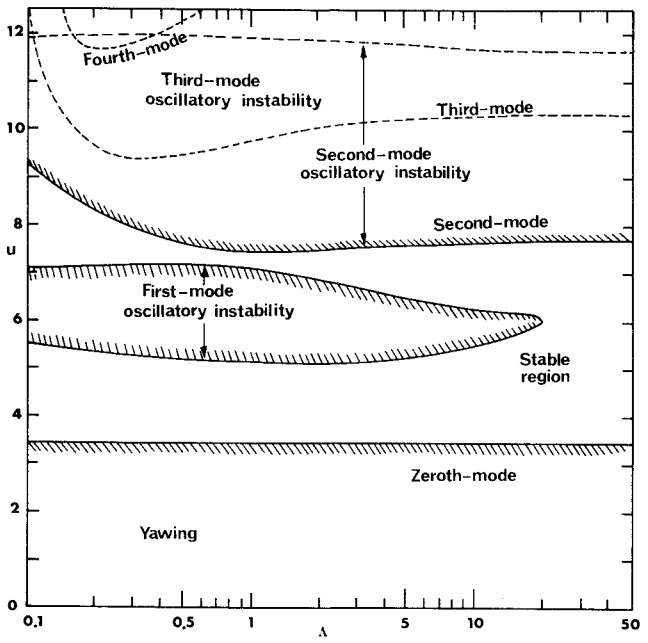

Fig. 7 Stability map showing the effect of Λ for a system with $\epsilon c_f = 1$, $\lambda_1 = 0.015$, $\alpha = 0.8$.

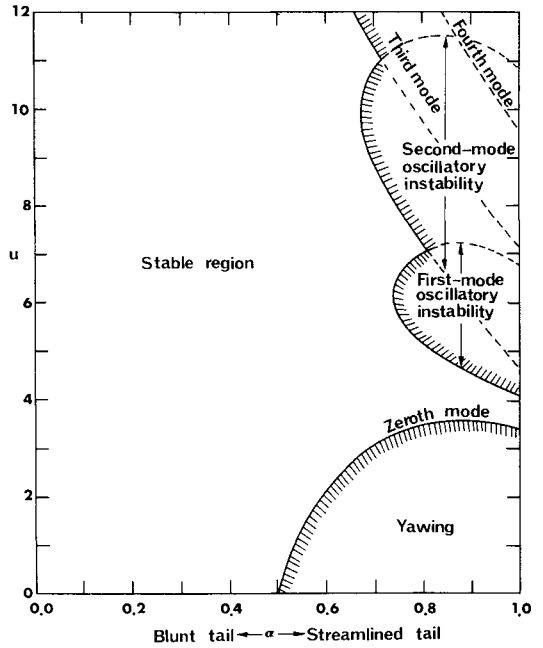

Fig. 8 Stability map showing the effect of the tail truncation ratio α, for a system with $\epsilon c_f = 1$, $\lambda_1 = 0.015$, and $\Lambda = 1$.

length (Λ) and the effect of shortening the tail (reducing α), for specific sets of the other parameters. It may be seen that making the tail more blunt is a far more effective means of stabilizing the system than is altering the tow-rope length.

Considering Fig. 7 in more detail, it is noted that yawing instability is independent of Λ, as found previously.[2,3] However, the system is more stable in terms of oscillatory instabilities if the tow-rope is sufficiently long or sufficiently short; indeed, the first-mode oscillatory instability entirely disappears at high enough Λ. It is also noted that these results differ considerably from those obtained previously.[2-4] This is mainly because the more of refined manner in which the tow-rope force was incorporated in this theory. Thus, the tow-rope force P_n is taken here to be $P_n = P_t(\partial\eta/\partial\xi - \eta/\Lambda)$, whereas previously it was simply taken as $P_n = -P_t(\eta/\Lambda)$. Clearly, although the latter is a reasonable approximation for short tow-ropes, it is inadequate for long tow-ropes.

Finally, the effect of slenderness of nose and tail were investigated. Figure 9 shows some results, for the second mode of the system, in which the nose and the tail were shortened by a factor of three, as compared to a "standard case" in which $\lambda_1 = 0.045$ and $\lambda_2 = 0.8\lambda_1 = 0.036$. It is seen that, if the nose is made shorter (but still ellipsoidal), the effect is to destabilize the system, whereas if the tail is made shorter, the opposite effect is obtained. It is noted that similar results were obtained in the case of the first mode of the system.

VI. Conclusion

The theory for the dynamics of towed flexible slender quasicylindrical bodies has been refined by obtaining the inviscid hydrodynamic forces acting on the nose and tail sections of the body by means of ideal-flow theory. At the same time, the tow-rope force was incorporated in a more refined manner. The analysis presented in the Appendix, giving the force and moment distributions on an ellipsoid

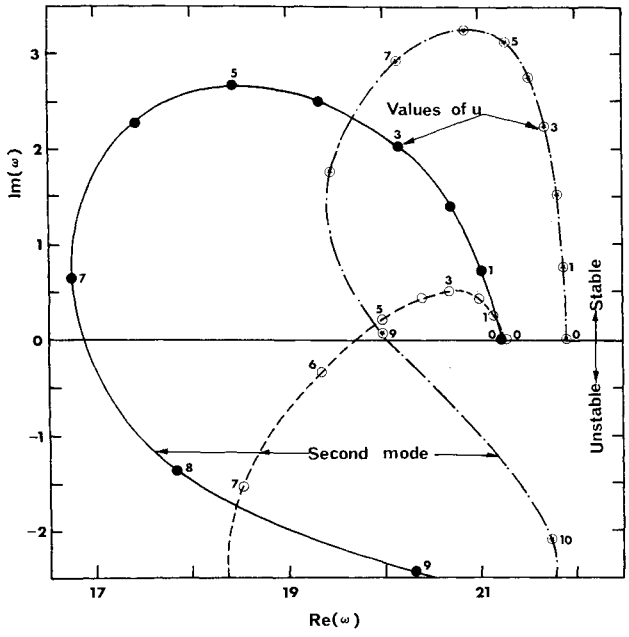

Fig. 9 The effect of nose and tail slenderness on stability for a system with $\epsilon c_f = 1$, $\Lambda = 1$, $\alpha = 0.8$. ——, $\lambda_1 = 0.045$, $\lambda_2 = 0.036$; —·—·—, $\lambda_1 = 0.045$, $\lambda_2 = 0.012$; ---, $\lambda_1 = 0.015$, $\lambda_2 = 0.036$.

undergoing plane motions, is quite general and may have wider interest than strictly in terms of the requirements of the paper.

Of course, this theory is a great deal more complex than the older theories.[2-4] However, the degree of complexity introduced is more than justified, particularly in view of the critical role on stability played by the forces acting at the two extremities of the towed body. This was borne out by the results obtained in this paper, where it was found that the dynamics of the system as predicted by this theory are considerably different from what was given by the older theories; although most of the results obtained here are qualitatively similar to those obtained previously, quantitative differences are quite important.

If one should wish to continue using the older theories, because of their simplicity, the work presented here offers, for the first time, the possibility of analytically determining the semiempirical factors associated with the inviscid hydrodynamic forces acting at the nose and tail of the body.

In terms of stability, it was shown that it is advantageous to tow a flexible body with either a very short or a very long tow-rope, a well-known result for rigid towed systems. However, from the practical point of view, this is not always possible; in any case, yawing (divergence) instability, if it occurs at all for a specific system, cannot be eliminated by manipulating the tow-rope length. A much more effective manner of stabilizing the system is by appropriate design of the nose and tail sections of the body. The nose should be as slender as possible – a desirable form in terms of towing efficiency in any case. The opposite applies to the tail, which should be nonslender and, if it has a truncated ellipsoidal shape, it should be truncated quite short; this theory provides the means for proper design to achieve overall stability.

Recent work on the effect of nose and tail shapes on stability of self-propelled articulated[5] and flexible systems, to be published in the near future, indicates that the previous findings apply to such systems also.

Appendix A: Force and Moment Distributions Along an Ellipsoid of Revolution Undergoing Plane Motion§

Lamb[10] investigated the net overall forces and moments exerted by fluid on a translating and rotating spheroid, but refrained from undertaking the "troublesome calculation of the effect of the fluid pressures on the surface of the solids." These troublesome calculations were carried out by Jones[11] for steady-state motion in a plane. Regrettably, Jones' failure to account for linear and angular accelerations renders his findings inadequate for our purposes.

§This work was conducted by the senior author in collaboration with P.J. Yoder, Research Assistant, McGill University.

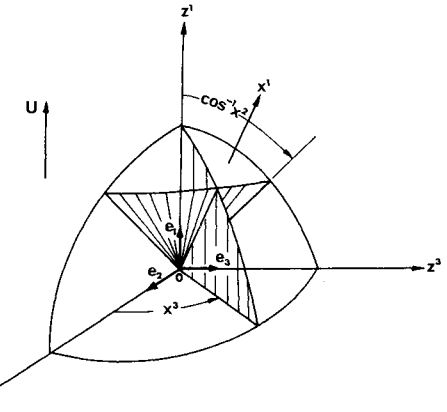

Fig. A1 The Cartesian and spheroidal coordinate systems used.

Let us introduce an inertial frame with Cartesian coordinates (Z^1,Z^2,Z^3), for which Bernoulli's equation applies

$$(p-p_\infty)/\rho = -\partial\phi/\partial t - \tfrac{1}{2}\nabla\phi\cdot\nabla\phi \tag{A1}$$

where p is the ambient pressure and ϕ is the velocity potential. In order to find ϕ for the ellipsoid, it is necessary to work in terms of coordinates which move with the body. We introduce, therefore, a second Cartesian system (z^1,z^2,z^3) embedded in the ellipsoid, whose origin coincides with the ellipsoid centroid, the z^1-axis pointing along the axis of the body.

If the ellipsoid has absolute translational and rotational velocities $V(t)$ and $\omega(t)$, respectively, then the velocity vectors of an arbitrary point moving in space corresponding to the fixed and moving coordinate systems $\dot{R}$ and $\dot{r}$, respectively, are related by

$$\dot{R}(t) = V(t) + \dot{r}(t) + \omega(t)\times r(t) \tag{A2}$$

where, for plane motions,

$$V = V^1 e_1 + V^2 e_2 \text{ and } \omega = \omega^3 e_3 \tag{A3}$$

the e_i being unit vectors of the z^i system (Fig. A1) Also consider a set of spheroidal coordinates (x^1,x^2,x^3) defined by the relations

$$\begin{aligned} z^1 &= aex^1x^2 \\ z^2 &= ae([x^1]^2-1)^{1/2}(1-[x^2]^2)^{1/2}\cos x^3 \\ z^3 &= ae([x^1]^2-1)^{1/2}(1-[x^2]^2)^{1/2}\sin x^3 \end{aligned} \tag{A4}$$

where $x^1 \geq 1$, $-1 \leq x^2 \leq 1$ and $0 \leq x^3 \leq 2\pi$(Fig. A1). The locus of points satisfying $x^1 = 1/e$ is a prolate spheroid, whose length is $2a$ and whose maximum radius is $b = a(1-e^2)^{1/2}$. The relation defining the surface of the spheroid is

$$F(x^i) = x^1 - 1/e = 0 \tag{A5}$$

Now, within the context of incompressible ideal flow theory, the equation of continuity is given by

$$\nabla^2\phi = 0 \tag{A6}$$

and the boundary conditions by

$$\nabla\phi \cdot \boldsymbol{n} = [\boldsymbol{V} + \boldsymbol{\omega} \times \boldsymbol{r}] \cdot \boldsymbol{n} \quad \text{on} \quad F(z^i) = 0 \tag{A7}$$

where $\boldsymbol{n}$ is a unit normal vector on the ellipsoid. The next step is to express Eqs. (A6) and (A7) in terms of spheroidal coordinates. For this purpose, the metric tensor g_{ij} and its reciprocal g^{ij} are introduced, $\boldsymbol{g}_i$ being the spheroidal unit vectors; one finds that

$$\boldsymbol{g}_1 = aex^2\boldsymbol{e}_1 + aex^1[f(x^2)/h(x^1)]^{1/2}\{\cos x^3\boldsymbol{e}_2 + \sin x^3\boldsymbol{e}_3\}$$

$$\boldsymbol{g}_2 = aex^1\boldsymbol{e}_1 - aex^2[h(x^1)/f(x^2)]^{1/2}\{\cos x^3\boldsymbol{e}_2 + \sin x^3\boldsymbol{e}_3\}$$

$$\boldsymbol{g}_3 = -ae[h(x^1)f(x^2)]^{1/2}\{\sin x^3\boldsymbol{e}_2 - \cos x^3\boldsymbol{e}_3\}$$

$$g_{11} = a^2e^2[h(x^1) + f(x^2)]/h(x^1)$$

$$g_{22} = a^2e^2[h(x^1) + f(x^2)]/f(x^2)$$

$$g_{33} = a^2e^2h(x^1)f(x^2) \text{ and } g_{ij} = 0 \text{ if } i \neq j$$

$$g^{ij} = 1/g_{ij} \text{ if } i = j \text{ and } g^{ij} = 0 \text{ if } i \neq j \tag{A8}$$

and

$$g = a^6e^6[h(x^1) + f(x^2)]^2$$

where

$$h(x^1) = ([x^1]^2 - 1)$$

and

$$f(x^2) = (1 - [x^2]^2)$$

Thus, Eq. (A6) may be written as

$$\nabla^2\phi = \frac{1}{(g)^{1/2}}\frac{\partial}{\partial x^i}\left(g^{1/2}g^{ij}\frac{\partial\phi}{\partial x^j}\right) = 0 \tag{A9}$$

Also,

$$\boldsymbol{n} = \frac{\nabla F}{|\nabla F|} = \frac{\boldsymbol{g}_1 g^{11}}{|\boldsymbol{g}_1 g^{11}|}\bigg|_{x^1 = 1/e} = \frac{\boldsymbol{g}_1}{(g_{11})^{1/2}}\bigg|_{x^1 = 1/e}$$

and hence, Eq. (A7) may be written as

$$\left[g_1g^{11}\frac{\partial\phi}{\partial x^1} + g_2g^{22}\frac{\partial\phi}{\partial x^2} + g_3g^{33}\frac{\partial\phi}{\partial x^3}\right] \cdot \frac{\boldsymbol{g}_1}{(g_{11})^{1/2}}$$

$$= [(V^1 - \omega^3z^2)\boldsymbol{e}_1 + (V^2 + \omega^3z^1)\boldsymbol{e}_2] \cdot \frac{\boldsymbol{g}_1}{(g_{11})^{1/2}}$$

$$\text{on } F = x^1 - 1/e = 0 \tag{A10}$$

where the various tensor quantities are given by Eq. (A8).

It is found that the potential found by Lamb[10] does satisfy Eqs. (A9) and (A10), i.e.,

$$\phi = -V^1ak_1(x^1)x^2 - V^2ae([x^1]^2 - 1)^{1/2}k_2(x^1)(1 - [x^2]^2)^{1/2}\cos x^3 - \omega^3a^2e([x^1]^2 - 1)^{1/2}\ell_3(x^1)x^2(1 - [x^2]^2)^{1/2}\cos x^3$$

where

$$-k_1(x^1) = \frac{e\left\{\frac{1}{2}x^1\log\frac{x^1+1}{x^1-1} - 1\right\}}{\left\{\frac{1}{2}\log\frac{1+e}{1-e} - \frac{e}{1-e^2}\right\}}$$

$$-k_2(x^1) = \frac{\left\{\frac{1}{2}\log\frac{x^1+1}{x^1-1} - \frac{x^1}{[x^1]^2-1}\right\}}{\left\{\frac{1}{2}\log\frac{1+e}{1-e^2} - \frac{e-2e^3}{1-e^2}\right\}} \tag{A11}$$

$$-\ell_3(x^1) = \frac{e^2\left\{3/2\, x^1\log\frac{x^1+1}{x^1-1} - 3 - \frac{1}{[x^1]^2-1}\right\}}{\left\{3/2\left(\frac{2-e^2}{e}\right)\log\frac{1+e}{1-e} - 6 + \frac{e^2}{1-e^2}\right\}}$$

Now rewriting Bernoulli's equation, Eq. (A1), in the form

$$(p - p_\infty)/\rho = \partial\phi/\partial t|_{r=\text{const}} + (\boldsymbol{V} + \boldsymbol{\omega} \times \boldsymbol{r}) \cdot \nabla\phi - \tfrac{1}{2}\nabla\phi \cdot \nabla\phi \tag{A12}$$

and substituting Eqs. (A11) and (A3) into it, after lengthy manipulation, one obtains

$$(p - p_\infty)/\rho = (\dot{V}^1c_{01} + \tfrac{1}{2}[V^1]^2c_{02}) + (\dot{V}^2c_{11} + V^1V^2c_{12} + \dot{\omega}^3c_{13} + \omega^3V^1c_{14})\cos x^3 + (\tfrac{1}{2}[V^2]^2c_{21} + \omega^3V^2c_{22} + \tfrac{1}{2}[\omega^3]^2c_{23})\cos^2 x^3 + (\tfrac{1}{2}[V^2]^2c_{31} + \omega^3V^2c_{32} + \tfrac{1}{2}[\omega^3]^2c_{33})\sin^2 x^3$$

where

$$c_{01} = ak_1x^2 \qquad \mathbf{c_{02}} = \mathbf{1} - \frac{(1+k_1)^2(1-[x^2]^2)}{1-e^2[x^2]^2}$$

$$c_{11} = bk_2(1-[x^2]^2)^{1/2}$$

$$c_{12} = \left(\frac{b}{a}\right)(1+k_1)(1+k_2)\frac{x^2(1-[x^2]^2)^{1/2}}{1-e^2[x^2]^2}$$

$$c_{13} = ab\ell_3x^2(1-[x^2]^2)^{1/2}$$

$$c_{14} = b\left\{\frac{(1+k_1)\{1+\ell_3(2[x^2]^2-1)\}}{1-e^2[x^2]^2} - 1\right\}(1-[x^2]^2)^{1/2}$$

$$c_{21} = 1 - \frac{(b/a)^2(1+k_2)^2[x^2]^2}{1-e^2[x^2]^2}$$

$$c_{22} = ax^2\left\{1 - \frac{(b/a)^2(1+k_2)\{1+\ell_3(2[x^2]^2-1)\}}{1-e^2[x^2]^2}\right\}$$

$$c_{23} = a^2[x^2]^2 + b^2(1-[x^2]^2) - \frac{b^2\{1+\ell_3(2[x^2]^2-1)\}^2}{1-e^2[x^2]^2}$$

$$c_{31} = 1 - (1+k_2)^2 \qquad c_{32} = ax^2\{1-(1+k_2)(1+\ell_3)\}$$

$$c_{33} = a^2[x^2]^2\{1-(1+\ell_3)^2\} \tag{A13}$$

$$k_i = k_i(x^1)|_{x^1=1/e},\ i = 1,2 \text{ and } \ell_3 = \ell_3(x^1)|_{x^1=1/e} \tag{A14}$$

Having determined the pressure, the force acting on the ellipsoid may be calculated i.e.,

$$\boldsymbol{F} = \iint_{\substack{\text{upper}\\ \text{sector}}} \frac{-p\boldsymbol{n}}{|\boldsymbol{n}.\boldsymbol{e}_3|}dz^2dz^1 + \iint_{\substack{\text{lower}\\ \text{sector}}} \frac{-p\boldsymbol{n}}{|\boldsymbol{n}.\boldsymbol{e}_3|}dz^2dz^1$$

but, since only the force per unit length along the ellipsoid axis is of interest, one need only determine

$$\frac{\partial F}{\partial z^1} = \int_{-b(1-[z^1/a]^2)^{1/2}}^{b(1-[z^1/a]^2)^{1/2}} -\frac{p\boldsymbol{n}}{|\boldsymbol{n}.\boldsymbol{e}_3|}dz^2 + \int_{b(1-[z^1/a]^2)^{1/2}}^{-b(1-[z^1/a]^2)^{1/2}} -\frac{p\boldsymbol{n}}{|\boldsymbol{n}.\boldsymbol{e}_3|}dz^2 \tag{A15}$$

Accordingly, substituting from Eq. (A13), keeping $z^1 = ax^2$ constant in the integration, and recalling that $x^1 = 1/e$ on the

ellipsoid, one obtains, after lengthy manipulation,

$$(\partial F/\partial z^1)\cdot e_1 = -\rho\pi(b^2/a)x^2$$
$$\times \{2\dot{V}^1 c_{01} + [V^1]^2 c_{02} + \tfrac{1}{2}[V^2]^2 (c_{21}+c_{31})$$
$$+\omega^3 V^2 (c_{22}+c_{32}) + \tfrac{1}{2}[\omega^3]^2 (c_{23}+c_{33})\} \qquad \text{(A16)}$$
$$(\partial F/\partial z^1)\cdot e_2 = -\rho\pi b\{\dot{V}^2 c_{11} + V^1 V^2 c_{12} + \dot{\omega}^3 c_{13} + \omega^3 V^1 c_{14}\}$$

and, in a similar manner, one obtains the moment

$$\frac{\partial \mathfrak{M}}{\partial z^1} = e_3 (z^1 - \frac{b^2}{a} x^2) \frac{\partial F}{\partial z^1}\cdot e_2 \qquad \text{(A17)}$$

These expressions may be used to obtain the forces acting per unit length on ellipsoidal nose or tail sections of a flexible body. Thus, for the nose section of the towed system under consideration, it is noted that

$$V^1 = -U \qquad \dot{V}^1 = 0$$
$$V^2 = U\frac{d\eta_1}{d\tau} + U\frac{d\theta_1}{d\tau}\left(\xi + \tfrac{1}{2}\right) + U\theta_1$$
$$\dot{V}^2 = \frac{U^2}{L}\frac{d^2\eta_1}{d\tau^2} + \frac{U^2}{L}\frac{d^2\theta_1}{d\tau^2}(\xi + \tfrac{1}{2}) + \frac{U^2}{L}\frac{d\theta_1}{d\tau}$$
$$\omega^3 = \frac{U}{L}\frac{d\theta_1}{d\tau} \qquad \dot{\omega}^3 = \frac{U^2}{L^2}\frac{d^2\theta_1}{d\tau^2} \qquad \text{(A18)}$$

where Eqs. (2) have been used and motions were assumed to be small. Substituting these into Eqs. (A16) and (A17), one obtains Eqs. (6). In a similar way, one may obtain Eqs. (7) for the tail section.

References

[1] Hawthorne, W.R., "The Early Development of the Dracone Flexible Barge," *Proceedings of Institution of Mechanical Engineers*, Vol. 175, 1961, pp. 52-83.

[2] Paidoussis, M.P., "Stability of Towed, Totally Submerged Flexible Cylinders," *Journal of Fluid Mechanics*, Vol. 34, 1968, pp. 273-297.

[3] Paidoussis, M.P., "Dynamics of Submerged Towed Cylinders," *Proceedings of the 8th Symposium on Naval Hydrodynamics*, Office of Naval Research, Arlington, Va., A.R.C. No. 179, 1970, pp. 981-1016.

[4] Pao, H.P., "Dynamical Stability of a Towed Thin Flexible Cylinder," *Journal of Hydronautics*, Vol. 4, Oct. 1970, pp. 145-150.

[5] Hamy, N., *The Trebron Sea Chain System,* Trebron Holdings Limited, ,Montreal, 1971.

[6] Taylor, G.I., "Analysis of the Swimming of Long and Narrow Animals," *Proceedings of Royal Society*, Vol. A214, 1952, pp. 158-183.

[7] Lighthill, M.J., "Note on the Swimming of Slender Fish," *Journal of Fluid Mechanics*, Vol. 9, 1960, pp. 305-317.

[8] Upson, R.H. and Klikoff, W.A., "Application of Practical Hydrodynamics to Airship Design," N.A.C.A. Rept. 405, 1931.

[9] Hoerner, S.F., *Fluid Dynamic Drag*, Published by author, Brick Town, N.J., 1965.

[10] Lamb, H., *Hydrodynamics*, Cambridge University Press, Cambridge, 1932.

[11] Jones, R., "Distribution of Normal Pressures on a Prolate Spheroid," Aeronautical Reseach Council, Reports and Memoranda 1061, 1927.